Available online at www.sciencedirect.com
ScienceDirect
Geochimica et Cosmochimica Acta 70 (2006) 4750–4769
Geochimica
www.elsevier.com/locate/gca

Partitioning and budget of Li, Be and B in high-pressure metamorphic rocks

Horst R. Marschall [a,*], Rainer Altherr [a], Thomas Ludwig [a], Angelika Kalt [b], Katalin Gméling [c], Zsolt Kasztovszky [c]

[a] *Mineralogisches Institut, Universität Heidelberg, Im Neuenheimer Feld 236, D-69120 Heidelberg, Germany*
[b] *Institut de Géologie, Université de Neuchâtel, Rue Emile Argand 11, CH-2007 Neuchâtel, Switzerland*
[c] *Institute of Isotopes, Hungarian Academy of Sciences, Konkoly Thege Miklós út 29–33, H-1121 Budapest, Hungary*

Received 18 November 2005; accepted in revised form 11 July 2006

Abstract

Partitioning and budget of Li, Be and B in high-pressure metamorphic rocks from the island of Syros (Greece) were studied, using secondary ion mass spectrometry, inductively coupled plasma optical emission spectrometry and prompt gamma neutron activation analysis. Partitioning between coexisting mineral phases was found to be rather constant and independent of element concentrations. For several mineral pairs, apparent partition coefficients vary in a narrow range, while concentrations vary by more than an order of magnitude. Hence, it was possible to establish sets of inter-mineral partition coefficients for Li, Be and B among 15 different high-pressure minerals. This data set provides important information on the behaviour of the light elements in different lithologies within subducting slabs from the onset of metamorphism to the eclogite stage. It is essential for modelling trace-element and isotope fractionation during subduction and dehydration of oceanic crust.

1. Introduction

The light elements Li, Be and B are important tracers for mass transfer in subduction zones. They are readily mobilised by fluids and melts and display strong isotope fractionation (Li and B) in nature. Concentrations of the three elements in the mantle and in fresh oceanic basalts are very low, whereas they are high in sediments, altered oceanic crust and continental crust. Therefore, any input of fluid or melt from the subducting slab into the overlying mantle has a strong impact on the light element budget and isotopic composition of the mantle wedge, and on the magmas generated there. Island arc volcanic rocks consequently display strong enrichments of Li, Be and B with respect to MORB (Ryan and Langmuir, 1987, 1988, 1993; Smith et al., 1997; Sano et al., 2001; Ryan, 2002) and specific Be and B isotopic signatures (Ishikawa and Nakamura, 1994; Ishikawa and Tera, 1997; Clift et al., 2001; Morris et al., 2002; Palmer and Swihart, 2002; Straub and Layne, 2002). Detailed knowledge on budget and partitioning of light elements within different materials of the subducting slab are essential for the modelling of Li, Be and B transfer and isotopic evolution in subduction zones. To fully understand the light element signatures of arc volcanic rocks, it is necessary to constrain quantitatively the behaviour of these elements during subduction-related progressive metamorphism of slab materials.

Recent work has been carried out on the bulk-rock Li, Be and B budgets of metasediments and metabasalts from subduction complexes and it was argued that substantial amounts of B and Li are liberated from the rocks during prograde metamorphism, while Be concentration does not vary significantly with metamorphic grade (Moran

* Corresponding author. Present address: Department of Earth Sciences, Wills Memorial Building, Queen's Road, University of Bristol, Bristol BS8 1RJ, UK. Fax: +44 117 9253385.
E-mail address: Horst.Marschall@bristol.ac.uk (H.R. Marschall).

0016-7037/$ - see front matter © 2006 Elsevier Inc. All rights reserved.
doi:10.1016/j.gca.2006.07.006

et al., 1992; Bebout et al., 1993, 1999; You et al., 1994; Peacock and Hervig, 1999; Zack et al., 2003). Studies on the partitioning behaviour of Li, Be and B between coexisting metamorphic minerals are scarce. Domanik et al. (1993) studied the fractionation of Be and B between minerals of metabasic and metasedimentary lithologies from the Catalina schists (California) and emphasised the importance of white mica stability on the Be and B budgets of subducting rocks. Woodland et al. (2002) studied the partitioning of Li between clinopyroxene and garnet in a large variety of eclogites and found that Li is preferentially incorporated in clinopyroxene. Zack et al. (2002) studied eclogites from Trescolmen (Central Swiss Alps) and found that Li and Be budgets are governed by clinopyroxene, while white mica and clinopyroxene control the B budget. Scambelluri et al. (2004) investigated B and Li concentrations in fluid inclusions and different minerals of serpentinites and olivine–orthopyroxene–chlorite rocks, and inferred a rather limited mobility of B and Li during the breakdown of serpentinites during subduction.

In this paper, abundances and corresponding partitioning data for Li, Be and B in various minerals of high-pressure metamorphic rocks from the Greek island of Syros (Cyclades) are reported. The major hosts of the light elements are identified, and the calculated whole-rock budgets are compared to the measured whole-rock abundances. A set of inter-mineral partition coefficients for the light elements Li, Be and B for 15 different H*P*-metamorphic minerals is presented. This dataset provides information on the behaviour of the light elements in different lithologies within subducting slabs. We demonstrate that a combination of the inter-mineral partition coefficients with clinopyroxene/fluid partition coefficients from experimental work Brenan et al. (1998b) can be used for the modelling of trace-element fractionation during subduction and dehydration of oceanic crust.

2. Analytical methods

Compositions of mineral phases were determined using a Cameca SX 51 electron microprobe equipped with five wavelength-dispersive spectrometers (Mineralogisches Institut, Heidelberg). Operating conditions were 20 nA beam current and 15 kV acceleration voltage. For analyses of phengite, the electron beam was defocused to 10 μm to avoid loss of alkalis. For analyses of tourmaline it was defocused to 5 μm. Details on counting times, crystals, standards and detection limits are given in Marschall (2005). PAP correction was applied to the raw data (Pouchou and Pichoir, 1984, 1985). For tourmaline, a modified matrix correction was applied, which is described in detail in Kalt et al. (2001).

Concentrations of Li, Be and B were measured by secondary ion mass spectrometry (SIMS) with a modified Cameca IMS 3f ion microprobe at the Mineralogisches Institut, Heidelberg, equipped with a primary beam mass filter. Analyses were performed using a 10 kV/20 nA $^{16}O^-$ primary ion beam. Positive secondary ions were accelerated through a nominal 4.5 kV. The energy window was set to 40 eV. We applied the energy filtering technique with an offset of 75 eV at a mass resolution $m/\Delta m$ (10%) of ~1000 to suppress interfering molecules and to minimise matrix effects (Ottolini et al., 1993). For all silicates, secondary ion intensities of ^{7}Li, ^{9}Be and ^{11}B were normalised to the count rate of ^{30}Si and calibrated against the NIST SRM 610 glass reference material using the concentrations of Pearce et al. (1997). The relative reproducibility was <1%. The accuracy is limited by matrix effects and the uncertainty of the element concentrations in the reference material. The accuracy is estimated to be <20% (Ottolini et al., 1993). Background near mass 11 was $\leqslant 10^{-2}$ cps ($\leqslant$1 ng/g). Results are not corrected for background. A 5-min pre-sputtering time was applied to each spot. For tourmaline, a modified setup was used, which is described in detail in Marschall et al. (2004).

Analyses of trace elements and especially of B at low concentration levels (<5 μg/g) are easily influenced by contamination on the surface of thin sections (Shaw et al., 1988; Domanik et al., 1993; Marschall and Ludwig, 2004). Therefore, the technique described by Marschall and Ludwig (2004) was applied to suppress the effect of contamination on trace element analysis using SIMS.

Whole-rock concentrations of Li in all samples were measured at the University of Bristol by ICP-OES (optical emission spectrometry), using a Jobin Yvon Ultima 2 Sequential Spectrometer, operated by Chung Choi (University of Bristol). Beryllium was analysed by Cavendish Analytical Laboratory Ltd., Canada, by ICP-OES. Details of sample preparation and applied analytical methods are given in Marschall (2005).

Whole-rock B concentrations were determined using prompt gamma neutron activation analysis (PGNAA) at the facility installed at the Budapest 10 MW research reactor, equipped with a cold neutron source (20 K). Thermal equivalent neutron flux at the target position is $\sim 5 \times 10^7$ per cm^2/s. The beam area was set to 4 cm^2, and exposure time was 1–4 h for most of the samples. Energy spectra ranging from 30 keV–11 MeV were measured using a high-purity germanium semiconductor (HPGe)—bismuth germanate (BGO) scintillator detector system in Compton-suppressed mode. The data acquisition was performed by a Canberra S100 multichannel analyser. Gamma spectra were evaluated using the Hypermet PC program (Révay et al., 2001).

Analytical details of the Budapest PGNAA facility are given in Révay et al. (2004), Szakmány and Kasztovszky (2004) and Molnár (2004), and references therein. Accuracy of B analyses by PGNAA has been checked by measurements of geological reference materials performed at Budapest Neutron Center (BNC) and is ~10% relative (Gméling et al., 2005). Precision is better than 1.5% relative for concentrations >5 μg/g and better than 1.7% relative in the range of low concentrations (1.9–5 μg/g). The calculated detection limit for B is 0.3 μg/g for the standard setup.

Further analytical details on PGNAA of high-pressure metamorphic rocks at BNC are given in Marschall et al. (2005).

3. Geology

The island of Syros displays a sequence of rocks of the lower unit of the Attic–Cycladic crystalline complex (ACCC). The major part of the island is composed of interlayered pelitic schists and marbles dipping N to NE (e.g. Hecht, 1984; Dixon and Ridley, 1987; Seck et al., 1996). The petrological, structural and tectono-metamorphic evolution of the island of Syros has been investigated in a large number of studies (Dixon, 1968; Bonneau et al., 1980; Ridley, 1982, 1984, 1986; Ballhaus and Schumacher, 1995; Trotet et al., 2001a; Rosenbaum et al., 2002; Ring et al., 2003; Brady et al., 2004; Keiter et al., 2004). For different rock types, a prograde P–T path was derived, characterised by a high P/T ratio, typical for subduction zone metamorphism. Metamorphic peak conditions were estimated at ~470–520 °C and 1.3–2.0 GPa (Dixon, 1968; Ridley, 1984; Okrusch and Bröcker, 1990; Trotet et al., 2001b; Rosenbaum et al., 2002; Keiter et al., 2004). The most interesting formations are exposed in the northern part of Syros near Kámpos and at the coastline around Hermoupolis and Kini. These formations are composed of metagabbros, eclogites, glaucophane schists, meta-plagiogranites, serpentinites and metasediments, which mainly preserve a blueschist- to eclogite-facies metamorphic overprint. They are interpreted as high-pressure metamorphic equivalents of different parts of ancient oceanic crust (e.g. Seck et al., 1996). Blocks of meta-igneous and meta-sedimentary rocks are embedded in a matrix of chlorite schist and serpentinite (Dixon, 1968; Hecht, 1984; Dixon and Ridley, 1987; Okrusch and Bröcker, 1990; Seck et al., 1996; Bröcker and Enders, 2001). Contacts between blocks and chemically and mineralogically contrasting matrix are characterised by blackwalls—reaction zones rich in OH-bearing minerals. The exhumation path of the Syros high-pressure rocks is characterised by near-isothermal decompression (Trotet et al., 2001b; Marschall et al., 2006). The lack of heating during exhumation resulted in the preservation of the H*P* assemblages and minerals in many places. Most of the blackwalls formed during exhumation and rehydration of the H*P* mélange (Marschall et al., 2006). Pressures between 0.6 and 0.75 GPa and temperatures of 400–430 °C were estimated for different blackwall samples (Marschall et al., 2006). Hence, the rock samples investigated in this study represent conditions including an extended pressure range between 0.6 and 2.0 GPa, but a limited temperature range of ~400–500 °C.

4. Investigated samples

Eight samples from high-pressure blocks and high-pressure metamorphic schists were investigated during this study, plus five samples from different blackwalls that formed during exhumation. A detailed description of all samples is given in an electronic Annex.

4.1. Metagabbros (SY344, SY438)

Sample SY344 is dominated by garnet and Ca-amphibole, the latter topotactically intergrown with glaucophane. All minerals are embedded in a matrix of epidote. Sample SY438 is dominated by glaucophane, phengite and lawsonite and minor clinopyroxene (omphacite).

4.2. Eclogites (SY109, SY323)

The investigated eclogites consist of garnet and clinopyroxene with minor epidote. SY109 contains additional white mica and glaucophane. SY308 is a *garnet–jadeite–quartz fels* (the term "fels" refers to an isotropic metamorphic rock) with minor amounts of glaucophane, epidote and paragonite.

4.3. Glaucophane schists (SY304, SY314, SY406)

The glaucophane schists are dominated by glaucophane, garnet and phengite that are accompanied by various additional phases, such as chloritoid (SY304) or tourmaline (SY314).

4.4. Quartz-rich vein (SY425D)

The quartz vein is crosscutting a metagabbro. This sample is characterised by euhedral clinozoisite, clinopyroxene and garnet, embedded in a matrix of quartz.

4.5. Schists from blackwalls (SY309B, SY325, SY328, SY404, SY441)

The blackwall samples consist of glaucophane + clinopyroxene + chlorite + epidote + tourmaline (SY309B), chlorite + talc + Ca-amphibole (SY325), clinopyroxene + chlorite + epidote (SY328), chlorite + titanite + apatite (SY404) and chlorite + tourmaline + titanite + clinopyroxene (SY441).

5. Modal rock compositions

Mass fractions of minerals (Table 1) are visual estimates combined with typical mineral densities. Only the fractions of phengite, titanite and tourmaline were calculated from bulk-rock concentrations of K_2O, TiO_2 and B_2O_3, respectively. For titanite, this procedure was only possible for rutile-free samples. Calculation of mass fractions of all minerals was not possible, because of major element zonations and similar chemical compositions of glaucophane and clinopyroxene.

Table 1
Estimated mass fractions of minerals in samples

Sample	Type	Cld	Ttn	Grt	Czo	Lws	Tur	Cpx	Cam	Gln	Chl	Tlc	Phe	Pg	Ab	Qtz	Other minerals
SY109	Eclogite		3	15	0.5			37		25			5.5	1		8	Rt, Zrn, Aln, Ap, Ilm
SY304	Gln schist	12		4	20					38	8		8.5	2nd		3	Rt, Ap
SY308	Meta-plagiogranite			6	4			21		5				25		38	Rt, Zrn, Ap
SY309B	Gln schist		0.3		2		11.8	20		36	25		0.1		2		Rt, Zrn, Aln, Ap
SY314	Gln schist		0.5	5	2.5		0.25			34			22		22	7	Ap, Mag
SY323	Eclogite		2	25	25		0.011	45							2nd	1	Rt, Zrn, Ap, Ilm
SY325	Tlc–Chl–Act schist								65		20	15					Rt
SY328	Omp–Chl fels[a]		0.5		6			60			20				2.5		Aln, Ap, Ilm, Mag, Py
SY344	Metagabbro		2	4	12			20	32	28			2.5				Ap
SY404	Chl schist		8								85						Rt, Aln, Ap, Py
SY406	Gln schist		0.5	35	2			4		38			19				Rt, Aln, Ap
SY425D	Qtz vein			5	20			5								70	
SY438	Metagabbro		1.5		5	10		5		59			18.5		2nd	1	
SY441	Chl schist		1.5				40	3			55						Ap

[a] The term "fels" refers to an isotropic metamorphic rock. Mass fractions (wt%) are visual estimates, which were controlled for some minerals by comparing whole-rock chemical analyses and electron microprobe mineral analyses. 2nd, secondary minerals formed during retrograde reactions. Mineral abbreviations after Kretz (1983): Cld, chloritoid; Ttn, titanite; Grt, garnet; Czo, clinozoisite (incl. epidote); Lws, lawsonite; Tur, tourmaline; Cpx, clinopyroxene (omphacite, jadeite); Cam, calcic amphibole; Gln, glaucophane; Chl, chlorite; Tlc, talc; Phe, phengite; Pg, paragonite; Ab, albite; Qtz, quartz; Rt, rutile; Zrn, zircon; Aln, allanite; Ap, apatite; Ilm, ilmenite; Mag, magnetite; Py, pyrite.

6. Li, Be and B concentrations in minerals

Mean, minimum and maximum abundances of Li, Be and B in the various minerals are given in Tables 2–4. Chloritoid, titanite, epidote/clinozoisite and quartz have very low concentrations of all three low-atomic mass elements. Fresh lawsonite in sample SY438 has very low abundances of Li and B (0.005 and 0.145 μg/g, respectively), whereas the concentration of Be is considerable (1.67 μg/g).

Garnet has highly variable concentrations of Li (0.152–5.97 μg/g), depending on bulk-rock composition, while B concentrations are very low (0.015–0.093 μg/g) and Be concentrations are generally near the detection limit of 0.001 μg/g. Small (<100 μm) garnet grains in samples SY314 and SY406 show strong zonation in Li with high contents (6–7 μg/g) in the cores and low contents (1–2 μg/g) in the rims. Garnet grains from all other samples are large (0.5–5 mm) and show (almost) no zonation in Li. The concentrations of B are nearly constant within all grains measured.

Tourmaline in sample SY314 has Li and Be concentrations of 8.6 and 0.37 μg/g, respectively, whereas concentrations in blackwall tourmaline (samples SY309B and SY441) are generally lower (2.1–5.3 μg/g Li; 0.041–0.055 μg/g Be). Profiles measured across large blackwall tourmaline grains show very constant Li and Be concentrations. B_2O_3 contents of 10.5–11.3 wt% result in 3.06–3.15 B cpfu, suggesting small amounts of tetrahedral B (Marschall et al., 2004).

Clinopyroxene has very high and variable concentrations of Li (6.81–130 μg/g) and Be (0.173–4.73 μg/g), but only minor concentrations of B (0.252–3.82 μg/g).

Ca-amphibole has low abundances of Li (0.976–1.30 μg/g) but relatively high abundances of both Be (0.662–4.34 μg/g) and B (2.98–9.16 μg/g). Glaucophane, similar to clinopyroxene, has very high concentrations of Li and Be and only minor concentrations of B. Lithium concentrations vary between 5.94 and 115 μg/g and are much higher than those of coexisting Ca-amphibole. On the other hand, the concentrations of Be in glaucophane range from 0.128 to 2.47 μg/g and are thus lower than those of the coexisting Ca-amphibole. Boron concentrations in glaucophane range from 0.226 to 6.96 μg/g, comparable to coexisting Ca-amphibole.

Phyllosilicates are characterised by highly variable light element abundances. Chlorite shows very high abundances of Li (3.45–115 μg/g), whereas those of Be and B are low, compared to other sheet silicates (Tables 2–4). Talc occurring in paragenesis with chlorite and Ca-amphibole (SY325) has relatively low contents of Li (0.433 μg/g) and Be (0.02 μg/g). Phengite has very high concentrations of all three elements (2.57–48.3 μg/g Li; 1.18–5.89 μg/g Be; 43–136 μg/g B), while paragonite has very high concentrations of Be and B and moderate Li concentrations (Tables 2–4). Beryllium concentrations in paragonite exceed those of all other silicates, and range from 2.74 to 15.6 μg/g, while B concentrations range from 20.2 to 117 μg/g. Lithium concentrations vary between 2.77 and 4.91 μg/g, and are higher than Li concentrations in coexisting phengite.

Albite has very low concentrations of Li (0.007–0.012 μg/g), moderate abundances of Be (0.461–0.527 μg/g) and low concentrations of B (0.307–1.35 μg/g).

7. Budgets of Li, Be and B

The budgets of Li, Be and B for representative samples are displayed in Fig. 1. The highest concentrations of Li were found in chlorite, glaucophane, clinopyroxene, phengite and paragonite. These phases contain more than 95% of

Table 2
Concentrations of Li in silicates (determined by SIMS) and whole-rock Li concentrations of investigated samples

Sample		Cld	Ttn	Grt	Czo	Lws	Tur	Cpx	Cam	Gln	Chl	Tlc	Phe	Pg	Ab	Qtz	WR_c	WR_m
SY109 Eclogite	Mean		n.a.	0.295	n.a.			8.06		7.17			2.57	4.91		<0.001	5.01	6.05
	1σ			0.078				0.36		0.28			0.34	1.51			1.00	0.37
	n			38				15		13			19	11		5		
SY304 Gln schist	Mean	<0.001		0.174	n.a.					9.95	11.9		2.71	(10.5)		0.007	5.50	7.75
	1σ			0.020						1.67	2.5		0.41	(3.4)		0.003	1.10	0.17
	n	5		7						14	13		9	12		4		
SY308 MPG[a]	Mean		n.a.	0.152	n.a.			6.81		5.94				2.77		<0.002	2.43	5.02
	1σ			0.077				0.32		1.27				1.27			0.49	0.18
	n			9				5		8				10		7		
SY309B Gln schist	Mean		0.030		0.545		2.10	27.2		41.0	34.7		5.85				29.2	31.7
	1σ		0.004		0.092		0.33	3.9		3.1	2.5		1.04				5.8	0.6
	n		6		5		33	17		19	16		21					
SY314 Gln schist	Mean		0.042	5.97	n.a.		8.59			94.0			45.9		0.007	n.a.	42.4	39.6
	1σ		0.023	0.92			2.70			16.9			9.3		0.004		8.5	0.8
	n		3	18			2			27			14		2			
SY323 Eclogite	Mean		0.042	3.47	1.11		n.a.	80.6							n.a.	n.a.	37.4	45.8
	1σ		0.007	0.81	0.40			18.1									7.5	0.9
	n		5	52	25			50										
SY325 Chl schist	Mean								1.30		3.45	0.433					1.60	2.29
	1σ								0.40		0.12	0.128					0.32	0.51
	n								46		10	11						
SY328 Omp–Chl fels	Mean		n.a.		0.436			65.4			115				0.012		62.3	65.3
	1σ				0.152			11.7			12				0.009		12.5	2.9
	n				10			30			21				4			
SY344 Metagabbro	Mean		n.a.	0.805	n.a.			24.7	0.976	30.6			9.71				14.1	18.8
	1σ			0.136				2.3	0.435	7.2			1.32				2.8	0.4
	n			37				29	26	29			10					
SY404 Chl schist	Mean		0.033								9.04						7.69	7.65
	1σ		0.006								0.83						1.54	0.14
	n		3								18							
SY406 Gln schist	Mean		n.a.	3.19	n.a.			130		115			49.3				59.4	66.7
	1σ			1.52				24		41			12.2				11.9	4.3
	n			38				17		35			26					
SY425D Qtz vein	Mean			1.06	0.220			59.7								0.067	3.17	3.30
	1σ			0.17	0.155			1.2								0.011	0.63	0.37
	n			18	5			6								7		
SY438 Metagabbro	Mean		0.048		n.a.	0.005		56.4		108			19.9			n.a.	70.2	88.7
	1σ		0.037			0.002		8.0		13			6.7				14.0	1.9
	n		2			13		4		9			8					
SY441 Chl schist	Mean		0.057				5.29	49.6			92						54.2	n.a.
	1σ		0.001					1.2			4						10.8	
	n		3				1	2			3							

[a] MPG, meta-plagiogranite. All concentrations in (μg/g). Numbers in parentheses refer to secondary mineral phases and were not used to calculate partition coefficients. The first row of each sample is mean concentration; the second row is standard deviation (1σ) of all analyses; the third row is the number of analyses (*n*) of this mineral in this sample. WR_c, whole-rock concentrations calculated by using mass fractions of minerals (Table 1) and Li concentrations of minerals (uncertainty of 20% assumed for estimations in mineral concentrations and mass fractions). WR_m, measured whole-rock concentrations. n.a., not analysed. Mineral abbreviations after Kretz (1983): Cld, chloritoid; Ttn, titanite; Grt, garnet; Czo, clinozoisite (incl. epidote); Lws, lawsonite; Tur, tourmaline; Cpx, clinopyroxene (omphacite, jadeite); Cam, calcic amphibole; Gln, glaucophane; Chl, chlorite; Tlc, talc; Phe, phengite; Pg, paragonite; Ab, albite; Qtz, quartz.

Table 3
Concentrations of Be in silicates (determined by SIMS) and whole-rock Be concentrations of investigated samples

Sample		Cld	Ttn	Grt	Czo	Lws	Tur	Cpx	Cam	Gln	Chl	Tlc	Phe	Pg	Ab	Qtz	WR_c	WR_m
SY109 Eclogite	Mean		n.a.	<0.003	n.a.			1.31		2.47			5.58	15.6		<0.001	1.57	1.77
	1σ							0.66		1.18			0.94	5.1			0.31	0.07
	n			6				15		13			19	11		5		
SY304 Gln schist	Mean	0.017		<0.001	n.a.					0.487	0.234		2.67	(2.95)		<0.001	0.58	0.46
	1σ	0.007								0.151	0.115		0.23	(1.52)			0.12	0.06
	n	11		7						14	13		18	12		4		
SY308 MPG[a]	Mean		n.a.	<0.001	n.a.			0.311		0.128				2.74		<0.001	0.76	0.82
	1σ							0.046		0.050				0.51			0.15	0.01
	n			9				5		8				10		7		
SY309B Gln schist	Mean		<0.002		0.030		0.041	2.38		0.812	0.295		4.11				0.85	0.65
	1σ				0.009		0.006	0.19		0.218	0.055		0.38				0.17	0.04
	n		6		5		33	17		19	16		21					
SY314 Gln schist	Mean		0.028	0.008	n.a.		0.37			1.59			5.67		0.527	n.a.	1.91	2.32
	1σ		0.008	0.004			0.30			1.25			0.48		0.342		0.38	0.04
	n		3	5			2			27			14		14			
SY323 Eclogite	Mean		<0.001	<0.004	0.046		n.a.	4.73							n.a.	n.a.	2.14	2.08
	1σ				0.030			2.38									0.43	0.02
	n		5	8	13			50										
SY325 Chl schist	Mean								4.34		0.357	<0.021					2.89	2.59
	1σ								1.08		0.047						0.58	0.03
	n								46		10	11						
SY328 Omp–Chl fels	Mean		n.a.		0.016			0.173			0.081				0.461		0.13	0.88
	1σ				0.010			0.113			0.030				0.057		0.03	0.03
	n				5			30			21				4			
SY344 Metagabbro	Mean		n.a.	<0.001	n.a.			0.285	0.662	0.390			1.18				0.41	0.54
	1σ							0.148	0.213	0.186			0.39				0.08	0.02
	n			13				29	26	29			10					
SY404 Chl schist	Mean		<0.001								0.350						0.3	0.91
	1σ										0.030						0.06	0.02
	n		3								18							
SY406 Gln schist	Mean		n.a.	0.012	n.a.			2.89		1.43			5.89				1.78	1.46
	1σ			0.013				0.65		0.41			1.55				0.36	0.2
	n			9				17		35			26					
SY425D Qtz vein	Mean			<0.001	0.020			1.25								<0.001	0.07	0.15
	1σ				0.007			0.15									0.01	0.02
	n			18	5			6								7		
SY438 Metagabbro	Mean		0.008		n.a.	1.67		3.02		1.59			4.74			n.a.	2.13	1.28
	1σ		0.003			0.74		0.75		0.95			3.37				0.4	0.03
	n		2			13		4		9			8					
SY441 Chl schist	Mean		<0.002				0.055	1.08			0.315						0.23	n.a.
	1σ							0.29			0.022						0.05	
	n		3				1	2			3							

[a] MPG, meta-plagiogranite. All concentrations in (μg/g). Numbers in parentheses refer to secondary mineral phases and were not used to calculate partition coefficients. The first row of each sample is mean concentration; the second row is standard deviation (1σ) of all analyses; the third row is the number of analyses of this mineral in this sample. WR_c, whole-rock concentrations calculated by using mass fractions of minerals (Table 1) and Be concentrations of minerals (uncertainty of 20% assumed for estimations in mineral concentrations and mass fractions). WR_m, measured whole-rock concentrations. n.a., not analysed. Mineral abbreviations after Kretz (1983): Cld, chloritoid; Ttn, titanite; Grt, garnet; Czo, clinozoisite (incl. epidote); Lws, lawsonite; Tur, tourmaline; Cpx, clinopyroxene (omphacite, jadeite); Cam, calcic amphibole; Gln, glaucophane; Chl, chlorite; Tlc, talc; Phe, phengite; Pg, paragonite; Ab, albite; Qtz, quartz.

Table 4
Concentrations of B in silicates (determined by SIMS) and whole-rock B concentrations of investigated samples

Sample		Cld	Ttn	Grt	Czo	Lws	Tur	Cpx	Cam	Gln	Chl	Tlc	Phe	Pg	Ab	Qtz	WR_c	WR_m
SY109 Eclogite	Mean		n.a.	0.024	n.a.			1.60		1.90			43.0	94.2		0.044	4.38	n.a.
	1σ			0.009				0.42		0.81			7.7	18.0		0.022	0.88	
	n			6				15		13			19	11		5		
SY304 Gln schist	Mean	0.014		0.024	n.a.					1.93	2.38		74.9	(117)		0.040	13.1	12.0
	1σ	0.010		0.004						0.42	0.90		4.9	(32)		0.033	2.6	0.2
	n	5		7						6	5		9	12		4		
SY308 MPG[a]	Mean		n.a.	0.015	n.a.			0.251		0.226				20.2		0.029	5.13	10.3
	1σ			0.005				0.057		0.092				6.3		0.014	1.03	0.1
	n			9				5		8				10		7		
SY309B Gln schist	Mean		0.030		0.478		33,623	1.92		5.53	1.47		136				3960	3960
	1σ		0.022		0.075		566	0.25		0.98	0.20		15					50
	n		4		5		33	17		19	8		14					
SY314 Gln schist	Mean		0.408	0.090	n.a.		31,496			1.43			66.3		0.307	n.a.	93.9	93.9
	1σ		0.134	0.031			404			0.96			6.0		0.120			1.2
	n		3	5			2			5			14		2			
SY323 Eclogite	Mean		0.046	0.093	0.273		n.a.	2.04							n.a.	n.a.	4.77	4.77
	1σ		0.018	0.041	0.097			0.39										0.06
	n		5	8	5			22										
SY325 Chl schist	Mean								9.16		1.92	4.77					7.05	7.15
	1σ								1.86		0.28	1.34					1.41	0.10
	n								46		10	11						
SY328 Omp–Chl fels	Mean		n.a.		0.609			3.82			2.50				1.35		2.86	7.58
	1σ				0.304			0.70			0.52				0.65		0.57	0.10
	n				5			5			5				4			
SY344 Metagabbro	Mean		n.a.	0.023	n.a.			1.52	2.98	3.99			48.2				3.58	5.05
	1σ			0.005				0.68	0.72	1.88			5.5				0.72	0.07
	n			13				29	26	29			10					
SY404 Chl schist	Mean		0.091								2.51						2.14	3.75
	1σ		0.014								0.47						0.43	0.06
	n		3								18							
SY406 Gln schist	Mean		n.a.	0.090	n.a.			2.70		3.92			86.9				18.1	18.2
	1σ			0.077				1.07		1.22			13.9				3.6	0.2
	n			9				17		35			26					
SY425D Qtz vein	Mean			0.040	0.221			0.824								0.027	0.11	1.90
	1σ			0.009	0.107			0.099								0.005	0.02	0.03
	n			18	5			6								7		
SY438 Metagabbro	Mean		0.149		n.a.	0.145		1.29		6.96			79.6			n.a.	18.9	19.6
	1σ		0.017			0.071		0.10		2.25			21.2				3.8	0.2
	n		2			13		4		9			8					
SY441 Chl schist	Mean		0.031				34,700	3.28			2.94						13,900	n.a.
	1σ		0.007					0.02			0.31						2800	
	n		3				1	2			3							

[a] MPG, meta-plagiogranite. All concentrations in (μg /g). Numbers in parentheses refer to secondary mineral phases and were not used to calculate partition coefficients. The first row of each sample is mean concentration; the second row is standard deviation (1σ) of all analyses; the third row is the number of analyses of this mineral in this sample. WR_c, whole-rock concentrations calculated by using mass fractions of minerals (Table 1) and B concentrations of minerals (uncertainty of 20% assumed for estimations in mineral concentrations and mass fractions). WR_m, measured whole-rock concentrations. n.a., not analysed. Mineral abbreviations after Kretz (1983): Cld, chloritoid; Ttn, titanite; Grt, garnet; Czo, clinozoisite (incl. epidote); Lws, lawsonite; Tur, tourmaline; Cpx, clinopyroxene (omphacite, jadeite); Cam, calcic amphibole; Gln, glaucophane; Chl, chlorite; Tlc, talc; Phe, phengite; Pg, paragonite; Ab, albite; Qtz, quartz.

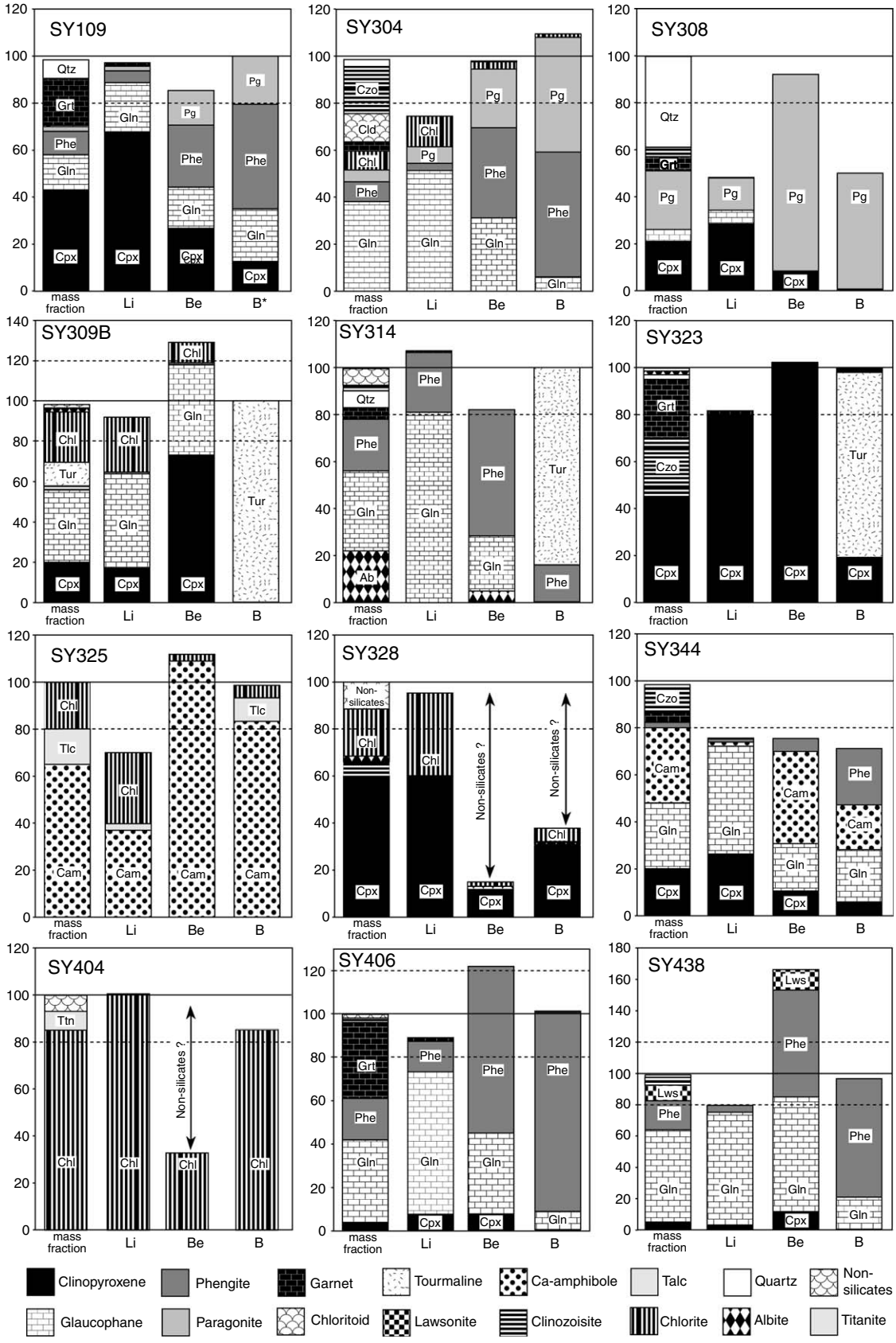

Fig. 1. Lithium, Be and B budgets of 12 samples. Every sample is shown in four columns for mass fraction of minerals, Li, Be and B contents, respectively, normalised to 100% of measured whole-rock contents. Uncertainties in calculation of the budgets are assumed to be 20% and are marked in all diagrams as dashed lines. *Boron whole-rock data for sample SY109 are not available; Boron budget for this sample is normalised to the calculated concentration of Table 4.

the Li budget of every sample investigated. Garnet, clinozoisite, tourmaline, Ca-amphibole and talc have only minor concentrations of Li. Chloritoid, titanite, lawsonite, quartz and albite are negligible for the Li budgets of the samples.

Beryllium contents are highest in paragonite, phengite, Ca-amphibole, clinopyroxene, lawsonite and glaucophane and much lower in albite and chlorite. All other phases are negligible for the Be budgets of the bulk rocks.

Apart from tourmaline, the most important hosts for B are paragonite and phengite, with B contents between 20 and 130 μg/g. All other phases have concentrations below 10 μg/g, with Ca-amphibole, talc, chlorite, glaucophane, clinopyroxene and albite between 0.2 and 9 μg/g. Nevertheless, these phases are important for the B budget of samples that have very low modal abundances of tourmaline and white micas (e.g. SY325 and SY344).

Lithium, Be and B budgets of the samples were calculated from mineral mass fractions (Table 1) and mean element concentrations (Tables 2–4). In most cases, calculated bulk-rock budgets of Li, Be and B are within 80–120% of the measured bulk-rock concentrations (Fig. 1). Only in a few cases are there significant differences between both values. In principle, these discrepancies could be due to (i) incorrect estimates of mineral mass fractions or (ii) incorporation of Li, Be and B in secondary and/or non-silicate minerals or in fluid inclusions.

8. Partitioning of Li, Be and B between high-pressure minerals

Equilibrium element partitioning between two phases depends on temperature, pressure and phase compositions. Temperatures during metamorphism were similar among samples and range from 400° to 500° (Okrusch and Bröcker, 1990; Trotet et al., 2001b; Marschall et al., 2006). However, as many mineral grains are chemically zoned, it is obvious that equilibrium was not attained. Nevertheless, the partitioning of Li, Be and B between the coexisting mineral phases was found to be rather constant and independent of element concentrations (Tables 5–7; Fig. 2). For almost all mineral pairs, apparent partition coefficients vary by less than one order of magnitude, for many of them by less than a factor of three, while concentrations vary by more than one order of magnitude.

Partitioning of trace elements between clinopyroxene and garnet is most relevant for eclogites. The partitioning of Li and B between these two phases is shown in Fig. 2a and b, respectively. Lithium concentrations range from 6.81 to 80.6 μg/g in clinopyroxene and from 0.152 to 3.47 μg/g in garnet, resulting in clinopyroxene/garnet partition coefficients between 23 and 56 with an average of 37 (Tables 2 and 5). Boron concentrations vary between 0.251 and 2.70 μg/g in clinopyroxene and between 0.015 and 0.090 μg/g in garnet. clinopyroxene/garnet partition coefficients for B range from 16 to 67 with an average of 37 (Tables 4 and 7). Beryllium concentrations in garnet are at or even below detection limit for most of the samples. Therefore, it is only possible to calculate a minimum clinopyroxene/garnet partition coefficient of 250 for Be (Table 6). The results show that in eclogitic lithologies, all three elements are strongly fractionated into clinopyroxene.

The partitioning of light elements between glaucophane and garnet (Fig. 2c and d) is very similar to that between clinopyroxene and garnet. Glaucophane and coexisting garnet from various samples show large variations in Li concentration (Table 2). Glaucophane/garnet partition coefficients for Li vary between 16 and 57 with an average of 35 (Table 5). In the case of B, variations in concentrations are smaller. Apparent partition coefficients show a relatively wide range from 15 to 170 (Table 7). Beryllium is concentrated in glaucophane, and the minimum partition coefficient is 160. All three elements are thus strongly fractionated into glaucophane.

Since phengite forms a significant constituent of many blueschists, the partitioning of light elements between glaucophane and phengite is of some importance. Observed Li concentrations in phengite vary between 2.57 and 49.3 μg/g (Table 2), resulting in glaucophane/phengite partition coefficients between 2.1 and 7.0 with an average of 3.8 (Table 5 and Fig. 2e). Beryllium concentrations in phengite range from 1.18 to 5.89 μg/g (Table 3) and glaucophane/phengite partition coefficients range from 0.18 to 0.44 with an average of 0.29 (Fig. 2f and Table 6). Measured B concentrations in phengite vary between 43.0 and 136 μg/g B (Table 4). The partition coefficient (glaucophane/phengite) is well defined between 0.022 and 0.088, with an average of 0.050 (Table 7 and Fig. 2g). These results show that Li is partitioned into glaucophane, Be is partitioned into phengite and B is almost exclusively fractionated into phengite.

Partitioning of Li, Be and B between clinopyroxene and glaucophane is shown in Fig. 2h, i and j, respectively. Lithium concentrations in both minerals show a wide range among different samples, as mentioned above. Clinopyroxene/glaucophane partition coefficients range from 0.52 to 1.15 with an average of 0.90 (Table 5). The partition coefficients for Be and B range from 0.5 to 2.9 (average 1.8) and from 0.19 to 1.11 (average 0.59), respectively (Tables 6 and 7). Note that partition coefficients between clinopyroxene and glaucophane of all three elements scatter around unity.

The partitioning of Li, Be and B between clinopyroxene and phengite is shown in Fig. 2k, l and m, respectively. Fig. 2k displays the large spread in Li concentrations in both clinopyroxene and phengite and shows a rather constant partition coefficient ranging from 2.6 to 4.7 with a mean of 3.2 (Table 5). The spread in Be concentrations is smaller and partition coefficients for Be vary between 0.23 and 0.64, with an average of 0.44 (Table 6). Boron concentrations in both minerals do not vary greatly. The partition coefficients range from 0.014 to 0.037, with an average of 0.026 (Table 7). The results show that Li partitions into clinopyroxene, while Be and B are preferentially incorporated into phengite.

Table 5
Partition coefficients of Li between 15 silicates, calculated from concentrations of Table 2

		Cld	Ttn	Grt	Czo	Lws	Tur	Cpx	Cam	Gln	Chl	Tlc	Phe	Pg	Ab	Qtz
Cld	Mean			>160						>8900	$>1.1\times10^{4}$		>2400			>6.6
	n			1						1	1		1			1
Ttn	Mean			110	22	0.096	120	1200		2000	1000		570		0.17	
	n			2	2	1	3	4		3	3		3		1	
	Min			80	18		70	800		1400	300		200			
	Max			140	26		200	1900		2300	1600		1090			
Grt	Mean	<0.0065	0.0097		0.26		1.4	37	1.2	35	69		12	17	0.0012	0.053
	n	1	2		2		1	6	1	6	1		5	2	1	2
	Min		0.0071		0.21			23		16			8	17		0.043
	Max		0.0122		0.32			56		57			16	18		0.064
Czo	Mean		0.046	4.0			3.9	140		75	160		11		0.027	
	n		2	2			1	4		1	2		1		1	
	Min		0.038	3.0				50			60					
	Max		0.055	4.8				270			260					
Lws	Mean		10					1.2×10^{4}		2.3×10^{4}			4300			
	n		1					1		1			1			
Tur	Mean		0.010	0.70	0.26			11		15	17		4.1		8.3×10^{-4}	
	n		3	1	1			2		2	2		2		1	
	Min		0.005					9		11	17		2.8			
	Max		0.014					13		20	17		5.3			
Cpx	Mean		9.1×10^{-4}	0.030	0.011	8.2×10^{-5}	0.092		0.040	1.2	1.6		0.33	0.51	1.8×10^{-4}	0.0011
	n		4	6	4	1	2		1	6	3		5	2	1	1
	Min		5.3×10^{-4}	0.018	0.004		0.077			0.9	1.3		0.22	0.41		
	Max		11.5×10^{-4}	0.043	0.020		0.107			1.9	1.9		0.34	0.61		
Cam	Mean			0.83						31	2.7	0.33	10			
	n			1						1	1	1	1			
Gln	Mean	$<1.1\times10^{-4}$	5.4×10^{-4}	0.034	0.013	4.3×10^{-5}	0.071	0.90	0.032		1.0		0.31	0.58	7.6×10^{-5}	7.4×10^{-4}
	n	1	3	6	1	1	2	6	1		2		7	2	1	1
	Min		4.5×10^{-4}	0.018			0.051	0.52			0.8		0.14	0.47		
	Max		7.3×10^{-4}	0.064			0.091	1.15			1.2		0.49	0.69		
Chl	Mean	$<9.4\times10^{-5}$	0.0017	0.015	0.0098		0.059	0.63	0.38	1.0		0.13	0.20		$1.0–10^{-4}$	6.2×10^{-4}
	n	1	3	1	2		2	3	1	2		1	2		1	1
	Min		0.0006		0.0038		0.058	0.54		0.8			0.17			
	Max		0.0037		0.0157		0.061	0.79		1.2			0.23			
Tlc	Mean								3.0		8.0					
	n								1		1					
Phe	Mean	$<4.2\times10^{-4}$	0.0028	0.091	0.093	2.3×10^{-4}	0.27	3.2	0.10	3.8	5.2			1.9	1.6×10^{-4}	0.0027
	n	1	3	5	1	1	2	5	1	7	2			1	1	1
	Min		0.0009	0.064			0.19	2.6		2.1	4.4					
	Max		0.0051	0.130			0.36	4.7		7.0	5.9					
Pg	Mean			0.058				2.1		1.8			0.52			$<6\times10^{-4}$
	n			2				2		2			1			2
	Min			0.055				1.6		1.5						
	Max			0.060				2.5		2.1						
Ab	Mean		5.9	840	37		1200			1.3×10^{4}	9700		6400			
	n		1	1	1		1			1	1		1			

(*continued on next page*)

Table 5 (*continued*)

		Cld	Ttn	Grt	Czo	Lws	Tur	Cpx	Cam	Gln	Chl	Tlc	Phe	Pg	Ab	Qtz
Qtz	Mean	<0.15		44	3.3			880		1400	1600		370	>1700		
	n	1		3	1			1		1	1		1	2		
	Min			16												
	Max			92												

Partition coefficients of Li between two minerals are ratios of concentrations (Li in mineral 1/Li in mineral 2). Mineral 1 is given in the top row, mineral 2 is given in the first column. The first row of each mineral is the Mean coefficient; the second row is the number of samples (*n*) used for calculation of partition coefficients (maximum or minimum values are given for cases in which one mineral shows concentrations below the detection limit). The third and fourth rows give minimum (min) and maximum (max) values for the partition coefficients. Mineral abbreviations after Kretz (1983): Cld, chloritoid; Ttn, titanite; Grt, garnet; Czo, clinozoisite (incl. epidote); Lws, lawsonite; Tur, tourmaline; Cpx, clinopyroxene (omphacite, jadeite); Cam, calcic amphibole; Gln, glaucophane; Chl, chlorite; Tlc, talc; Phe, phengite; Pg, paragonite; Ab, albite; Qtz, quartz.

The examples discussed above show that in the high-pressure metamorphic rocks from Syros, partitioning of Li, Be and B between coexisting minerals is systematic. Partition coefficients vary by a factor of two or three in most examples and they are independent of absolute concentrations. Only in some cases, such as the partitioning of B between garnet and other phases, the partition coefficients vary by more than one order of magnitude. This unusually large variation may be due to analytical uncertainties at very low concentration levels of B in garnet, or due to slow diffusion of B in garnet.

In many blueschist- and eclogite-facies high-pressure metamorphic rocks, clinopyroxene is a major host for Li and Be, and it also incorporates some B. The partitioning of Li, Be and B between clinopyroxene and melt and clinopyroxene and aqueous fluid has been studied experimentally (Brenan et al., 1998a,b). Therefore, in the following discussion, clinopyroxene is used as a reference mineral. Mineral/clinopyroxene partition coefficients for Li, Be and B calculated from the observed mineral/mineral partition coefficients (Tables 5–7) are presented in Fig. 3. The results for Li show that almost all mineral/clinopyroxene partition coefficients are smaller than unity, except for glaucophane (1.2 ± 0.6) and chlorite (1.6 ± 0.3). For Be, actinolite/clinopyroxene and glaucophane/clinopyroxene partition coefficients are near to unity, while the respective partition coefficients of white micas and albite are clearly above unity. For B, phengite/clinopyroxene and paragonite/clinopyroxene partition coefficients are very high (45 and 70, respectively) and those for the amphiboles, chlorite and talc are close to unity.

9. Discussion

In the following discussion, the budgets of Li, Be and B in progressively metamorphosed subducting oceanic crust are discussed and a model is presented, which can be used to estimate the mobilisation of the light elements during dehydration. Li, Be and B are strongly fractionated among different minerals in H*P* metamorphic rocks. Very high concentrations of lithium are found in the major phases of chlorite schists, glaucophane schists, metagabbros and eclogites, namely chlorite, glaucophane and clinopyroxene. Thus, the major phases are the principal carriers of Li and are able to incorporate large amounts of Li into their crystal structures. Therefore, Li has the potential to stay in the rocks during prograde high-pressure metamorphism of altered oceanic crust. At low metamorphic grades, Li can be hosted in chlorite, and during formation of blueschists, it will enter glaucophane. Later on, the blueschist-eclogite transition is characterised by continuous reactions occurring over certain *P*–*T* ranges. During this process, the modal abundance of glaucophane decreases, while the amount of clinopyroxene increases, until finally an eclogite assemblage dominated by clinopyroxene and garnet will form. As described above, the clinopyroxene structure is able to incorporate large amounts of Li and, therefore, a large por-

Table 6
Partition coefficients of Be between 15 silicates, calculated from concentrations of Table 3

		Cld	Ttn	Grt	Czo	Lws	Tur	Cpx	Cam	Gln	Chl	Tlc	Phe	Pg	Ab	Qtz
Cld	Mean			<0.03						29	14		160			<0.02
	n			1						1	1		1			1
Ttn	Mean			0.30	>10	210	22	390		130	>160		400		19	
	n			1	2	1	3	1		2	3		2		1	
	Min						13			60			200			
	Max						30			200			610			
Grt	Mean	>30	3.4		>10		44	250	>900	160	>500		590	>4000	63	d.l.
	n	1	1		2		1	1	1	2	1		2	1	1	4
	Min									120			510			
	Max									190			680			
Czo	Mean			<0.1			1.4	64		27	7.5		140		30	<0.02
	n			2			1	4		1	2		1		1	1
	Min							11			5.2					
	Max							103			9.8					
Lws	Mean		0.0047					1.8		0.95			2.8			
	n		1					1		1			1			
Tur	Mean		0.077	0.023	0.73			39		12	6.4		58		1.4	
	n		1	1	1			2		2	2		2		1	
	Min							20		4	5.7		15			
	Max							58		20	7.2		100			
Cpx	Mean		0.0013	0.0020	0.032	0.55	0.034		2.3	0.84	0.30		2.8	10	2.7	<0.002
	n		4	6	4	1	2		1	6	3		5	2	1	3
	Min		0.0003	0.0005	0.010		0.017			0.34	0.12		1.6	9		
	Max		0.0026	0.0024	0.090		0.051			1.89	0.47		4.3	12		
Cam	Mean			<0.001				0.43		0.59	0.082	<0.005	1.8			
	n			1				1		1	1	1	1			
Gln	Mean	0.035	0.0083	0.0037	0.037	1.1	0.14	1.8	1.7		0.42		3.8	14	0.33	<0.005
	n	1	3	6	1	1	2	6	1		2		7	2	1	3
	Min		0.0023	0.0010			0.05	0.5			0.36		2.3	6		
	Max		0.0177	0.0081			0.23	2.9			0.48		5.5	21		
Chl	Mean	0.072	<0.006	<0.002	0.15		0.16	4.5	12	2.4		<0.06	13		5.7	<0.002
	n	1	3	1	2		2	3	1	2		1	2		1	1
	Min				0.10		0.14	2.1		2.1			11			
	Max				0.19		0.18	8.1		2.8			14			
Tlc	Mean								>200		>20					
	n								1		1					
Phe	Mean	0.0063	0.0024	9.4×10^{-4}	0.0074	0.35	0.038	0.44	0.56	0.29	0.080			2.8	0.093	$<1 \times 10^{-4}$
	n	1	3	5	1	1	2	5	1	7	2			1	1	2
	Min		0.0005	1.8×10^{-4}			0.010	0.23		0.18	0.072					
	Max		0.0050	19.6×10^{-4}			0.065	0.64		0.44	0.088					
Pg	Mean			1.9×10^{-4}				0.099		0.10			0.36			$<3 \times 10^{-4}$
	n			1				2		2			1			2
	Min							0.084		0.05						
	Max							0.114		0.16						
Ab	Mean		0.054	0.016	0.034		0.70	0.38		3.0	0.18		11			
	n		1	1	1		1	1		1	1		1			
Qtz	Mean	>40		>1	>60			>400		>200	>600		>7000	>4000		
	n	1		4	1			3		3	1		2	2		

Partition coefficients of Be between two minerals are ratios of concentrations (Be in mineral 1/Be in mineral 2). Mineral 1 is given in the top row, mineral 2 is given in the first column. The first row of each mineral is the mean coefficient; the second row is the number of samples (*n*) used for calculation of partition coefficients (maximum or minimum values are given for cases in which one mineral shows concentrations below the detection limit; d.l., both minerals below detection limit). The third and fourth rows give minimum (min) and maximum (max) values for the partition coefficients. Mineral abbreviations after Kretz (1983): Cld, chloritoid; Ttn, titanite; Grt, garnet; Czo, clinozoisite (incl. epidote); Lws, lawsonite; Tur, tourmaline; Cpx, clinopyroxene (omphacite, jadeite); Cam, calcic amphibole; Gln, glaucophane; Chl, chlorite; Tlc, talc; Phe, phengite; Pg, paragonite; Ab, albite; Qtz, quartz.

Table 7
Partition coefficients of B between 14 silicates, calculated from concentrations of Table 4

		Cld	Ttn	Grt	Czo	Lws	Cpx	Cam	Gln	Chl	Tlc	Phe	Pg	Ab	Qtz
Cld	Mean			1.7					140	170		5300			2.8
	n			1					1	1		1			1
Ttn	Mean			1.1	11	0.97	56		79	57		1800		0.75	
	n			2	2	1	4		3	3		3		1	
	Min			0.2	6		9		35	28		160			
	Max			2.0	16		104		186	94		4600			
Grt	Mean	0.60	2.5		4.3		37	130	68	100		1800	2600	3.4	1.5
	n	1	2		2		6	1	6	1		5	2	1	4
	Min		0.5		2.9		16		15			700	1300		0.7
	Max		4.5		5.6		67		170			3200	4000		1.9
Czo	Mean		0.12	0.26			5.4		12	3.6		280		2.2	0.12
	n		2	2			4		1	2		1		1	1
	Min		0.06	0.18			3.7			3.1					
	Max		0.17	0.34			7.5			4.1					
Lws	Mean		1.0				8.9		48			550			
	n		1				1		1			1			
Cpx	Mean		0.041	0.037	0.20	0.11		2.0	2.4	0.77		45	70	0.35	0.059
	n		4	6	4	1		1	6	3		5	2	1	3
	Min		0.010	0.015	0.13				0.9	0.66		27	59		0.027
	Max		0.116	0.061	0.27				5.4	0.90		71	81		0.116
Cam	Mean			0.0079					1.3	0.21	0.52	16			
	n			1					1	1	1	1			
Gln	Mean	0.0074	0.10	0.031	0.087	0.021	0.59	0.75		0.75		25	70	0.21	0.058
	n	1	3	6	1	1	6	1		2		7	2	1	3
	Min		0.01	0.006			0.19			0.27		11	50		0.021
	Max		0.29	0.068			1.11			1.23		46	90		0.129
Chl	Mean	0.006	0.022	0.010	0.28		1.3	4.8	2.3		2.5	62		0.54	0.017
	n	1	3	1	2		3	1	2		1	2		1	1
	Min		0.011		0.24		1.1		0.8			32			
	Max		0.036		0.33		1.5		3.8			92			
Tlc	Mean							1.9		0.4					
	n							1		1					
Phe	Mean	1.9×10^{-4}	0.0028	7.5×10^{-4}	0.0035	0.0018	0.026	0.062	0.050	0.021			2.2	0.0046	7.8×10^{-4}
	n	1	3	5	1	1	5	1	7	2			1	1	2
	Min		0.0002	3.2×10^{-4}			0.014		0.022	0.011					5.4×10^{-4}
	Max		0.0062	13.6×10^{-4}			0.037		0.088	0.032					10.2×10^{-4}
Pg	Mean			5.1×10^{-4}			0.015		0.016			0.46			9.5×10^{-4}
	n			2			2		2			1			2
	Min			2.5×10^{-4}			0.012		0.011						4.7×10^{-4}
	Max			7.6×10^{-4}			0.017		0.020						14.4×10^{-4}
Ab	Mean		1.3	0.30	0.45				4.7	1.9		220			
	n		1	1	1				1	1		1			
Qtz	Mean	0.35		0.78	8.2		25		33	59		1400	1400		
	n	1		4	1		3		3	1		2	2		
	Min			0.53			9		8			1000	700		
	Max			1.47			36		48			1900	2200		

Partition coefficients of B between two minerals are ratios of concentrations (B in mineral 1 /B in mineral 2). Mineral 1 is given in the top row, mineral 2 is given in the first column. The first row of each mineral is the mean coefficient; the second row is the number of samples (*n*) used for calculation of partition coefficients (maximum or minimum values are given for cases in which one mineral shows concentrations below the detection limit). The third and fourth rows give minimum (min) and maximum (max) values for the partition coefficients. Mineral abbreviations after Kretz (1983): Cld, chloritoid; Ttn, titanite; Grt, garnet; Czo, clinozoisite (incl. epidote); Lws, lawsonite; Cpx, clinopyroxene (omphacite, jadeite); Cam, calcic amphibole; Gln, glaucophane; Chl, chlorite; Tlc, talc; Phe, phengite; Pg, paragonite; Ab, albite; Qtz, quartz.

tion of the rock's Li could be retained within the eclogite. Woodland et al. (2002) have shown that metabasaltic eclogites from different localities and metamorphic grade have significant whole-rock Li concentrations of up to 31 μg/g, most of which is hosted in clinopyroxene. Furthermore, Zack et al. (2002, 2003) report whole-rock Li contents of eclogites from Trescolmen (Central Alps) reaching 41 μg/g and Hermann (2002) reports Li contents of 46 and 102 μg/g in two phengite-bearing eclogites from Dora Maira (Western Alps).

Beryllium is mainly hosted in clinopyroxene, glaucophane and white mica; in addition, Ca-amphibole, lawsonite and albite may also contain significant amounts of Be. As discussed above for Li, Be should also be retained

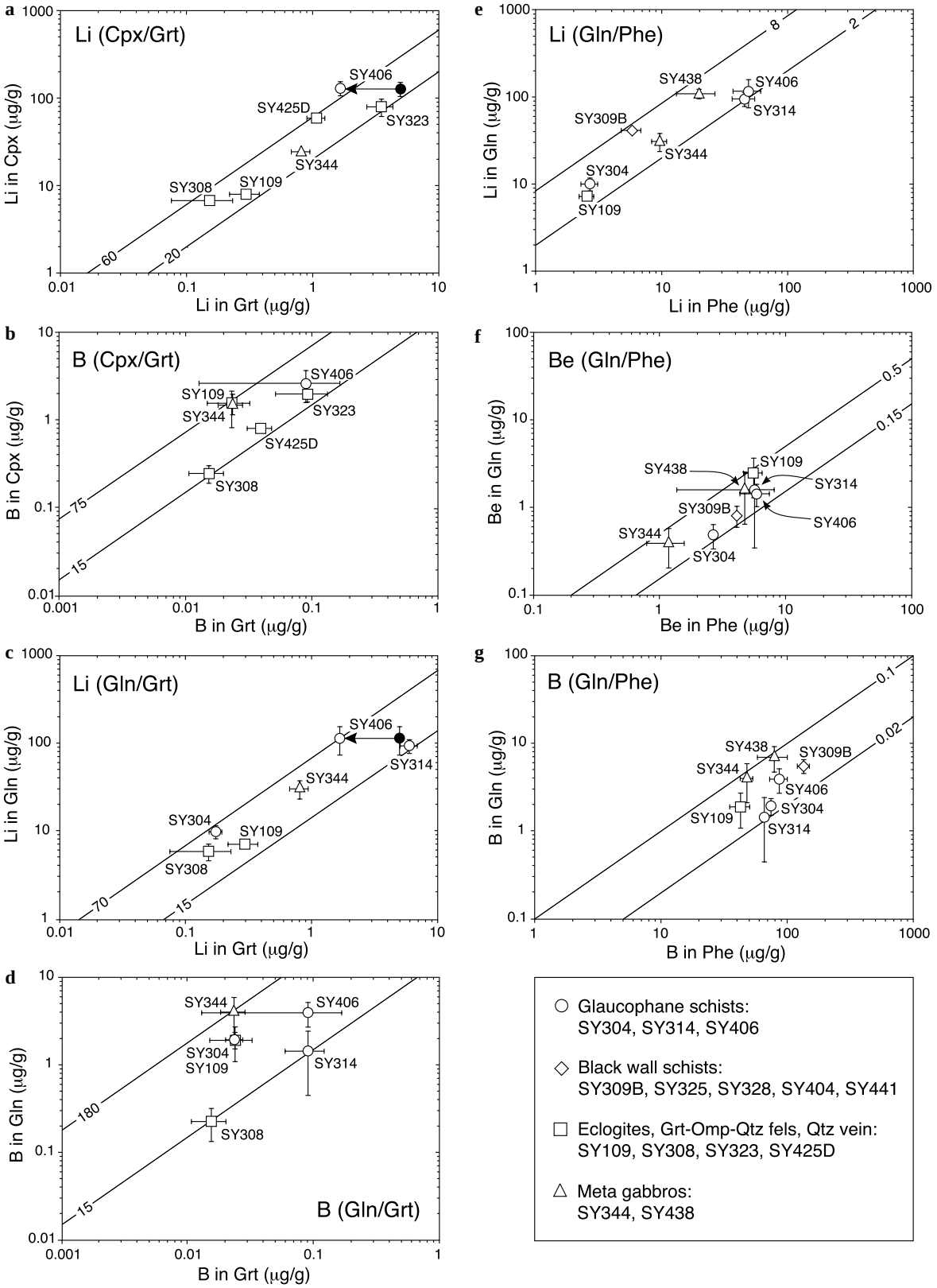

Fig. 2. (a–d) Concentrations of Li (a and c) and B (b and d) in coexisting clinopyroxene-garnet (a and b) and glaucophane-garnet (c and d) pairs. Garnet in sample SY406 is zoned in Li with decreasing concentrations from core (filled cycle) to rim (open cycle). (e–g) Concentrations of (e) Lithium, (f) Beryllium and (g) Boron in coexisting glaucophane–phengite pairs in various samples. (h–j) Concentrations of Li, Be and B in coexisting clinopyroxene–glaucophane pairs. (k–m) Concentrations of Li, Be and B in coexisting clinopyroxene–phengite pairs. Diagonal lines mark constant partition coefficients (values given on lines). Circles, glaucophane schists; diamonds, black wall schists; squares, eclogites; and triangles, meta gabbros. Note that not all mineral pairs occur in each samples, and therefore, not all samples are plotted in each diagram.

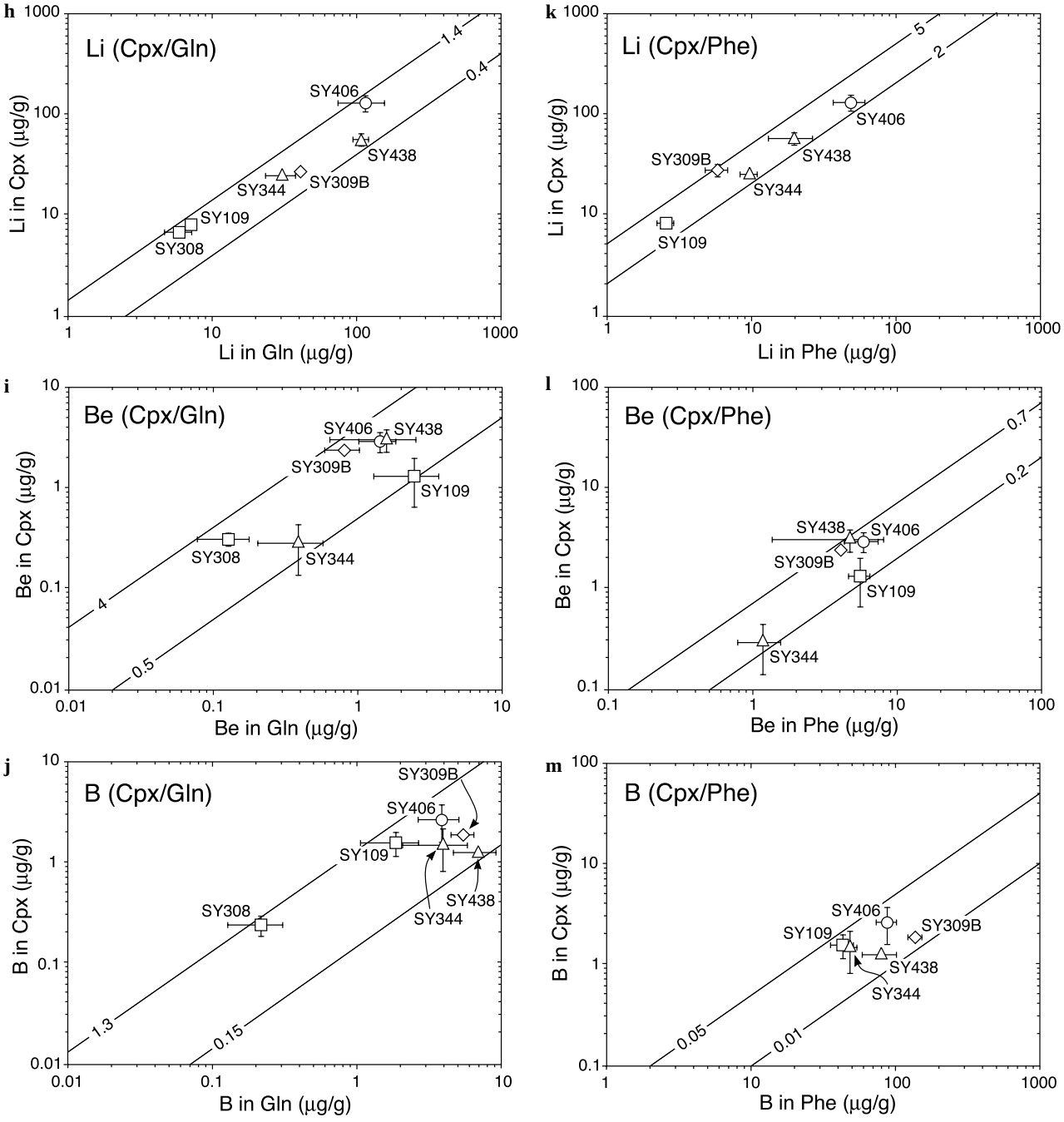

Fig. 2 (*continued*)

in progressively dehydrating rocks of the subducting oceanic crust. It will be hosted by Ca-amphibole and albite in greenschists, by glaucophane and white mica in blueschists and by clinopyroxene in eclogites. Domanik et al. (1993) found white mica to contain the highest concentrations of Be in high-pressure rocks, which is in agreement with the results presented here. However, the limited modal abundance of white mica compared to glaucophane and clinopyroxene limits the importance of phengite and paragonite for the Be budgets of the rocks. Zack et al. (2002) underlined the importance of clinopyroxene as the principal carrier of Be in eclogites, which is in agreement with the results obtained in this study.

During our investigation special emphasis was put on analyses of boron at low concentration levels (Marschall and Ludwig, 2004). This turned out to be very important, as almost all of the investigated minerals contain less than 10 µg/g B and most contain even less than 1 µg/g. The only minerals (except for tourmaline) showing higher concentrations of B are phengite and paragonite. Previous studies demonstrated that white micas are important carriers of B in high-pressure rocks (Domanik et al., 1993; Hermann,

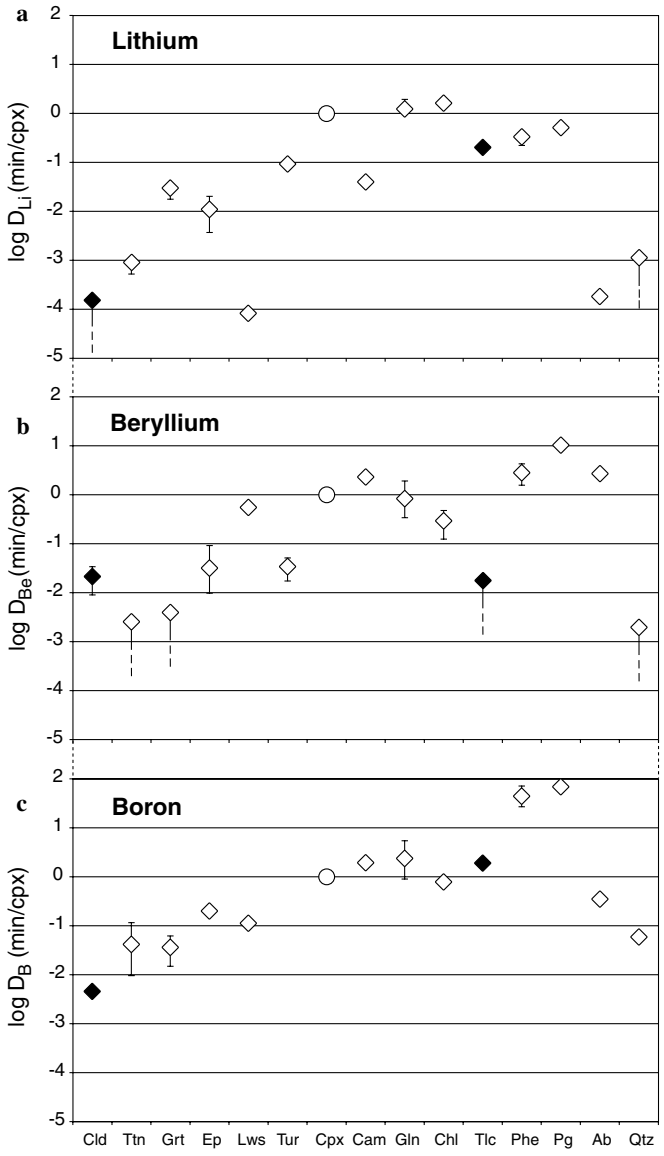

Fig. 3. Mineral/clinopyroxene partition coefficients of (a) Lithium, (b) Beryllium and (c) Boron for 15 different H*P* metamorphic minerals plotted as log $D^{mineral/Cpx}$. Minerals are arranged in the order of increasing silicate polymerisation. Open diamonds display minerals for which partition coefficients were directly calculated from concentration ratios between the respective mineral and coexisting clinopyroxene. Black diamonds display minerals which were not observed in equilibrium with clinopyroxene. *D* values for these minerals were calculated by combining clinopyroxene/chlorite with mineral/chlorite concentration ratios. Open circle represents clinopyroxene.

2002; Zack et al., 2002). However, these studies were not focused on accuracy of B measurements at low concentration levels and, therefore, might have overestimated the concentrations of B in minerals coexisting with white mica, namely clinopyroxene, amphibole and garnet. Overestimation of B at low concentration levels leads to partition coefficients between white mica and coexisting minerals that are too low. The measurements presented here revealed relatively low concentrations in minerals coexisting with B-rich white micas, resulting in high partition coefficients ($D^{Phe/Cpx} = 45$; $D^{Pg/Cpx} = 70$; Table 5). The latter underline the importance of phengite and paragonite as hosts of B. The contribution of phases other than phengite, paragonite and tourmaline to the B budget of H*P* metamorphic rocks is smaller than formerly thought. In contrast to the results of Domanik et al. (1993) who measured 5–55 μg/g B in lawsonite, our measurements of Syros lawsonite reveals only 0.145 μg/g B (SY438; Table 4) in equilibrium with B-rich phengite in a B-rich rock (Table 4). Lawsonite has much lower B concentrations than the coexisting clinopyroxene and glaucophane. Therefore, the role of lawsonite as an important carrier of B in high-pressure metamphic rocks has to be negated on the basis of our results. Analyses of chlorite during this study showed that surface contamination is a serious problem, especially for sheet silicates. The highest concentrations of B in chlorite from six different samples are only between 2.50 and 2.95 μg/g and are almost two orders of magnitude lower than B concentrations of coexisting paragonite (Table 4). Therefore, chlorite must be recognised as only a minor host of B. Our analyses of Syros rocks also revealed very low B concentrations in garnet (15–93 ng/g), making garnet insignificant for the B budget of garnet–glaucophanites and eclogites, even at high modes, which is in contrast to earlier studies (e.g. Zack et al., 2002). The significantly higher apparent B concentrations reported in previous studies using SIMS or LA-ICP-MS techniques may be explained by surface contamination of thin sections or by small mineral and fluid inclusions, which were not recognisable during analysis.

Tomascak et al. (2002) discussed Li, Be and B contents and Li isotopic compositions of basalts and andesites from different island arcs. They found that volcanic rocks enriched in B (high B/Be) demonstrate neither a significant enrichment in Li nor a subduction-related Li isotope signature. The authors emphasise a strong discrepancy between the fluid-mobile character of Li and its lack of enrichment in arc magmas. This apparent contradiction is solved by assuming that Mg-silicates of the mantle wedge may act as a filter. Fluids released from the dehydrating slab are thought to contain high concentrations of Li and B. Experimental studies on the trace-element mobility in fluids (as well as supercritical fluids and melts) released from eclogites at ultra-high pressures (4–6 GPa) by Kessel et al. (2005) have revealed much lower eclogite/fluid partition coefficients for B than for Li for a wide temperature range. The partitioning of Li and B between peridotite and hydrous fluid at high pressures and temperatures is also significantly different from each other, with $D^{peridotite/fluid} \approx 0.01$ for B and ≈0.1 for Li (Brenan et al., 1998b). Consequently, B should be transferred through the mantle wedge to the magma source region, while Li should be stripped from the fluids by Mg-silicates in the mantle peridotite directly overlying the subducting plate. Paquin and Altherr (2002) and Paquin et al. (2004) have demonstrated that the ultrahigh-pressure garnet peridotite from Alpe Arami (Central Swiss Alps) was subjected to a

subduction-related Li metasomatism without a concomitant significant enrichment in B. They argued that clinopyroxene and olivine of the lower and colder parts of the mantle remove slab-derived Li from fluids migrating from the dehydrating slab into the hot regions of subarc melting. B, in contrast, is not significantly incorporated by these minerals, due to its low mineral/fluid partition coefficients for mantle minerals (e.g. Brenan et al., 1998b). However, other studies suggest that partition coefficients of Li, Be and B between olivine–orthopyroxene assemblages and hydrous fluids may not differ significantly from each other (Scambelluri et al., 2004; Tenthorey and Hermann, 2004).

Table 8
Partition coefficients of Li, Be and B between 15 silicates and fluid

	Li	Be	B
Chloritoid	2.4×10^{-5}	0.039	7.4×10^{-5}
Titanite	1.5×10^{-4}	2.3×10^{-3}	6.6×10^{-4}
Garnet	4.8×10^{-3}	3.6×10^{-3}	5.9×10^{-4}
Clinozoisite	1.8×10^{-3}	0.058	3.2×10^{-3}
Lawsonite	1.3×10^{-5}	0.99	1.8×10^{-3}
Tourmaline	0.015	0.061	—
Clinopyroxene[a]	0.16	1.8	0.016
Ca-amphibole	6.4×10^{-3}	4.1	0.032
Glaucophane	0.19	1.5	0.038
Chlorite	0.26	0.54	0.012
Talc	0.033	0.032	0.031
Phengite	0.053	5.0	0.72
Paragonite	0.082	18	1.1
Albite	2.9×10^{-5}	4.9	5.6×10^{-3}
Quartz	1.8×10^{-4}	3.6×10^{-3}	9.4×10^{-4}

[a] Cpx/Fluid data from Brenan et al. (1998b). No B value for the borosilicate tourmaline was calculated.

Modelling trace-element mobility during dehydration of the subducting slab requires knowledge on the partition behaviour of elements between H*P* metamorphic rocks and released fluids. Brenan et al. (1998b) combined experimentally determined Li, Be and B partition coefficients between clinopyroxene (and garnet) and aqueous fluid (pure water and 0.5 M HCl at 2.0 GPa and 900 °C) with mineral/clinopyroxene partition coefficients determined on natural H*P* metamorphic rocks (Domanik et al., 1993), and derived mineral/fluid partition coefficients for five different H*P* minerals (Grt, Cpx, Lws, Am and mica). Whole rock/fluid partition coefficients were derived from modal composition of MORB + H_2O during progressive subduction (Poli and Schmidt, 1995). Using this method, Brenan et al. (1998b) showed that B/Be ratios of rocks and fluid in subducting hydrous MORB strongly decrease during the first ~60 km of subduction. Our study contributes information on the partitioning and budget of Li, Be and B for a broader range of H*P* metamorphic minerals, which can be used in the same way for a quantitative calculation of light element release. Table 8 shows mineral/fluid partition coefficients derived from the combination of inter-mineral partition coefficients (Tables 5–7) with mineral/clinopyroxene partition coefficients (Brenan et al., 1998b). Fig. 4a shows the modal composition of a hypothetical metabasalt at three different stages of dehydration, from greenschist (~5 wt% H_2O), to blueschist (~1.5 wt% H_2O) to a phengite-bearing eclogite (~0.1 wt% H_2O). The release of trace elements during each step of dehydration is modelled by using the calculated whole-rock/fluid partition coefficients, and the amount of released H_2O. In Fig. 4b the modelled Li, Be and B concentrations are shown for the progressive dehydration from a pre-metamorphic

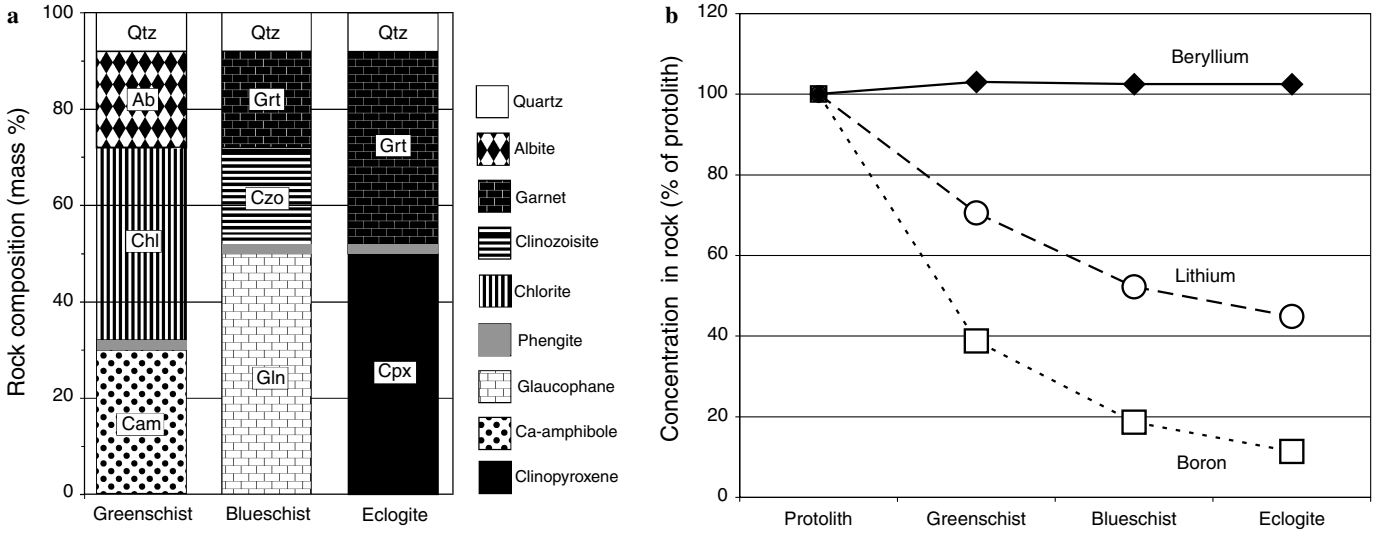

Fig. 4. (a) Modal composition of a hypothetical metabasalt at three different metamorphic stages, i.e. greenschist, blueschist and eclogite facies. (b) Modelled Li, Be and B concentrations of the sequence of rocks displayed in (a) plotted relative to the initial element concentrations. Note that Be concentrations are almost constant (or slightly increase due to the loss of H_2O), while Li and B concentrations decrease to levels of ~45% and ~10%, respectively. The abundances were calculated using whole rock/fluid partition coefficients derived from the modal rock compositions in combination with mineral/fluid partition coefficients (Table 8). H_2O concentrations of the rocks were calculated from stoichiometric concentrations in the minerals.

protolith (~10 wt% H_2O) through the three metamorphic stages displayed in Fig. 4a. The results show that Be concentrations are unaffected by the metamorphic dehydration. Lithium is decreased to ~45% of the initial value, and only ~10% of the boron is preserved in the eclogite. The results suggest that Li much stronger than B may be retained in the subducting oceanic crust itself, and thus, half of the lithium may not even be mobilised. Hence, the retention of Li in eclogitic clinopyroxene probably also contributes to the fractionation of the fluid-mobile elements Li and B. A more quantitative examination of fluid transport and fractionation of the light elements and their isotopes will be discussed in a separate paper.

Formation and stability of tourmaline will immobilise B and will cause a quantitative retention of B in the subducting material. Preferential incorporation of B in white mica shows that this element is hosted by the same minerals as are K, Rb, Ba, Cs (LILE) in high-pressure metamorphic rocks (Domanik et al., 1993; Sorensen et al., 1997; Melzer and Wunder, 2000; Zack et al., 2001; Schmidt et al., 2004). Therefore, in the absence of tourmaline, a white mica-bearing oceanic crust will show coupled B-LILE systematics during subduction. In contrast, high-pressure dravite has very low concentrations of LILE (Marschall, 2005), whereas B is a major component of this mineral, with concentrations of ~3 wt% B. Formation of tourmaline will thus lead to a decoupling of B from LILE (K, Rb, Ba, and Cs).

10. Conclusions

All three elements Li, Be and B are strongly fractionated among different H*P* minerals. Very high concentrations of lithium occur in chlorite, glaucophane and clinopyroxene and to a lesser extent in paragonite and phengite. Beryllium is mainly hosted by clinopyroxene, glaucophane and white mica. In addition, Ca-amphibole, lawsonite and albite may also contain considerable amounts of Be. The only minerals (except for tourmaline) showing B concentrations in excess of 10 μg/g are phengite and paragonite.

This study presents a set of inter-mineral partition coefficients for the light elements Li, Be and B for 15 H*P* metamorphic minerals, derived from in-situ analyses of coexisting phases in different natural rock samples. This data set provides important information on the behaviour of the light elements in different lithologies within subducting slabs in the depth region between the onset of subduction and the stability field of eclogites. Also, it is essential for modelling trace-element and isotope fractionation during subduction and dehydration of oceanic crust. The calculated model presented here demonstrates that much more lithium than boron will be retained in the metabasalts, which may contribute to the fractionation of the two fluid mobile elements in subduction zones. Modelling of Li, Be and B mobilisation and isotope fractionation will be presented in greater detail in a separate paper.

Acknowledgments

The authors thank Hans-Peter Meyer for microprobe maintenance and for providing mineral formula calculation programs. This paper benefited from discussions with Stefan Prowatke, Jens Paquin and Thomas Zack. Emily Lowe helped to improve the English style. Ilona Fin and Oliver Wienand are thanked for preparing high-quality thin sections for electron and ion microprobe investigation. Chung Choi is thanked for performing ICP-OES analyses. The paper benefited from positive and constructive reviews by Thomas Pettke, Bill Leeman and Roberta Rudnick, and editorial handling by Rick Ryerson, which is greatly acknowledged. This study resulted from the Dr. rer. nat. thesis of H.M. and was financially supported by the Deutsche Forschungsgemeinschaft (DFG, Grants KA 1023/8-1 and AL 166/15-3), which is greatly acknowledged. PGNAA and ICP-OES work was financed by the European Community Access to Research Infrastructure framework, Contract HPRI-1999-CT-00099, awarded to G.L. Molnár, and Contract HPRI-1999-CT-00008, awarded to B.J. Wood.

Associate editor: F.J. Ryerson

Appendix A. Supplementary data

Supplementary data associated with this article can be found, in the online version, at doi:10.1016/j.gca.2006.07.006.

References

Alt, J.C., 1995. Subseafloor processes in mid-ocean ridge hydrothermal systems. In: *Seafloor Hydrothermal Systems: Physical, Chemical, Biological, and Geological Interactions*. In: Humphris, S.E. (Ed.), *Geophys. Monogr. Ser*, Vol. 91. Am. Geophys. Union, Washington, DC, pp. 85–114.

Ballhaus, C., Schumacher, J.C., 1995. Stratigraphy, deformation and high-pressure metamorphism of the island of Syros (Cyclades, Greece). *Bochumer Geologische und Geotechnische Arbeiten* **44**, 13–16.

Bebout, G.E., Ryan, J.G., Leeman, W.P., 1993. B–Be systematics in subduction-related metamorphic rocks: characterization of the subducted component. *Geochim. Cosmochim. Acta* **57**, 2227–2237.

Bebout, G.E., Ryan, J.G., Leeman, W.P., Bebout, A.E., 1999. Fractionation of trace elements by subduction-zone metamorphism—effect of convergent-margin thermal evolution. *Earth Planet. Sci. Lett.* **171**, 63–81.

Bonneau, M., Geyssant, J., Kienast, J.R., Lepvrier, C., Maluski, H., 1980. Tectonique et métamorphisme Haute Pression d'âge éocène dans les Hellénides: exemple de l'île de Syros (Cyclades, Grèce). *C.R. Acad. Sci., Paris, Sér. D* **291**, 171–174.

Brady, J.B., Markley, M.J., Schumacher, J.C., Cheney, J.T., Bianciardi, G.A., 2004. Aragonite pseudomorphs in high-pressure marbles of Syros. *Greece, J. Struct. Geol.* **26**, 3–9.

Brenan, J.M., Neroda, E., Lindstrom, C.C., Shaw, H.F., Ryerson, F.J., Phinney, D.L., 1998a. Behavior of boron, beryllium and lithium during melting and crystallization: constraints from mineral–melt partitioning experiments. *Geochim. Cosmochim. Acta* **62**, 2129–2141.

Brenan, J.M., Ryerson, F.J., Shaw, H.F., 1998b. The role of aqueous fluids in the slab-to-mantle transfer of boron, beryllium, and lithium during subduction: experiments and models. *Geochim. Cosmochim. Acta* **62**, 3337–3347.

Bröcker, M., Enders, M., 2001. Unusual bulk-rock compositions in eclogite-facies rocks from Syros and Tinos (Cyclades, Greece): implications for U–Pb zircon geochronology. *Chem. Geol.* **175**, 581–603.

Clift, P.D., Rose, E.F., Shimizu, N., Layne, G.D., Draut, A.E., Regelous, M., 2001. Tracing the evolving flux from the subducting plate in the Tonga–Kermadec arc system using boron in volcanic glass. *Geochim. Cosmochim. Acta* **65**, 3347–3364.

Dixon, J.E., 1968. The metamorphic rocks of Syros, Greece, Ph.D. thesis, St. John's College, Cambridge.

Dixon, J.E., Ridley, J., 1987. Syros. In: *Chemical Transport in Metasomatic Processes*. In: Helgeson, H.C. (Ed.), *NATO ASI Series C, Math. Phys. Sci*, Vol. 218. Reidel, Dordrecht, pp. 89–501.

Domanik, K.J., Hervig, R.L., Peacock, S.M., 1993. Beryllium and boron in subduction zone minerals: an ion microprobe study. *Geochim. Cosmochim. Acta* **57**, 4997–5010.

Gméling, K., Szabolcs, H., Kasztovszky, Zs., 2005. Boron and chlorine concentration of volcanic rocks: an application of prompt gamma activation analysis. *J. Radioanal. Nucl. Chem.* **265**, 201–214.

Hecht, J., 1984. *Geological map of Greece 1:50,000, Syros island*. Institute of Geology and Mineral Exploration, Athens.

Hermann, J., 2002. Allanite: thorium and light rare earth element carrier in subducted crust. *Chem. Geol.* **192**, 289–306.

Ishikawa, T., Nakamura, E., 1994. Origin of the slab component in arc lavas from across-arc variation of B and Pb isotopes. *Nature* **370**, 205–208.

Ishikawa, T., Tera, F., 1997. Source, composition and distribution of the fluid in the Kurile mantle wedge: constraints from across-arc variations of B/Nb and B isotopes. *Earth Planet. Sci. Lett.* **152**, 123–138.

Kalt, A., Schreyer, W., Ludwig, T., Prowatke, S., Bernhardt, H.-J., Ertl, A., 2001. Complete solid solution between magnesian schorl and lithian excess-boron olenite in a pegmatite from the Koralpe (eastern Alps, Austria). *Eur. J. Mineral.* **13**, 1191–1205.

Keiter, M., Piepjohn, K., Ballhaus, C., Bode, M., Lagos, M., 2004. Structural development of high-pressure metamorphic rocks on Syros island (Cyclades, Greece). *J. Struct. Geol.* **26**, 1433–1445.

Kessel, R., Schmidt, M.W., Ulmer, P., Pettke, T., 2005. Trace element signature of subduction-zone fluids, melts and supercritical liquids at 120– 180 km depth. *Nature* **437**, 724–727.

Kretz, R., 1983. Symbols for rock-forming minerals. *Am. Mineral.* **68**, 277–279.

Marschall, H.R., 2005. Lithium, beryllium, and boron in high-pressure metamorphic rocks from Syros (Greece), Dr. rer. nat. thesis, Univ. Heidelberg, Germany, <http://www.ub.uni-heidelberg.de/archiv/5634>.

Marschall, H.R., Ludwig, T., 2004. The Low-Boron contest: minimising surface contamination and analysing boron concentrations at the ng/g-level by secondary ion mass spectrometry. *Mineral. Petrol.* **81**, 265–278.

Marschall, H.R., Ertl, A., Hughes, J.M., McCammon, C., 2004. Metamorphic Na- and OH-rich disordered dravite with tetrahedral boron, associated with omphacite, from Syros, Greece: chemistry and structure. *Eur. J. Mineral.* **16**, 817–823.

Marschall, H.R., Kasztovszky, Zs., Gméling, K., Altherr, R., 2005. Chemical analysis of high-pressure metamorphic rocks by PGNAA—comparison with results from XRF and solution-ICP-MS. *J. Radioanal. Nucl. Chem.* **265**, 339–348.

Marschall, H.R., Ludwig, T., Altherr, R., Kalt, A., Tonarini, S., 2006. Syros metasomatic tourmaline: evidence for very high-δ^{11}B fluids in subduction zones. *J. Petrol.* in press, doi:10.1093/petrology/eg1031.

Melzer, S., Wunder, B., 2000. Island-arc basalts alkali ratios: constraints from phengite–fluid partition experiments. *Geology* **28**, 583–586.

Molnár, G.L., 2004. *Handbook of Prompt Gamma Activation Analysis with Neutron Beams*. Kluwer Academic Publishers, Dordrecht.

Moran, A.E., Sisson, V.B., Leeman, W.P., 1992. Boron depletion during progressive metamorphism: implications for subduction processes. *Earth Planet. Sci. Lett.* **111**, 331–349.

Morris, J.D., Gosse, J., Brachfeld, S., Tera, F., 2002. Cosmogenic Be-10 and the solid Earth: studies in geomagnetism, subduction zone processes, and active tectonics. In: *Beryllium: Mineralogy, Petrology and Geochemistry*. In: Grew, E.S. (Ed.), *Rev. Mineral.*, vol. 50. Mineral. Soc. Am., Washington, DC, pp. 207–270, Chapter 5.

Okrusch, M., Bröcker, M., 1990. Eclogites associated with high-grade blueschists in the Cyclades archipelago, Greece: a review. *Eur. J. Mineral.* **2**, 451–478.

Ottolini, L., Bottazzi, P., Vannucci, R., 1993. Quantification of lithium, beryllium and boron in silicates by secondary ion mass spectrometry using conventional energy filtering. *Anal. Chem.* **65**, 1960–1968.

Palmer, M.R., Swihart, G.H., 2002. Boron isotope geochemistry: an overview. In: *Boron: Mineralogy, Petrology and Geochemistry*, second ed.. In: Grew, E.S., Anovitz, L.M. (Eds.), *Rev. Mineral.*, Vol. 33 Mineral. Soc. Am., Washington, DC, pp. 709–744, Chapter 13.

Paquin, J., Altherr, R., 2002. Subduction-related lithium metasomatism during exhumation of the Alpe Arami ultrahigh-pressure garnet peridotite (Central Alps, Switzerland). *Contibs. Mineral. Petrol.* **143**, 623–640.

Paquin, J., Altherr, R., Ludwig, T., 2004. Li–Be–B systematics in the ultrahigh-pressure garnet peridotite from Alpe Arami (Central Swiss Alps): implications for slab-to-mantle transfer. *Earth Planet. Sci. Lett.* **218**, 507–519.

Peacock, S.M., Hervig, R.L., 1999. Boron isotopic composition of subduction-zone metamorphic rocks. *Chem. Geol.* **160**, 281–290.

Pearce, N.J.G., Perkins, W.T., Westgate, J.A., Gorton, M.P., Jackson, S.E., Neal, C.R., Chenery, S.P., 1997. A compilation of new and published major and trace element data for NIST SRM 610 and NIST SRM 612 glass reference materials. *Geostand. Newsl.* **21**, 115–144.

Poli, S., Schmidt, M.W., 1995. H_2O transport and release in subduction zones: experimental constraints on basaltic and andesitic systems. *J. Geophys. Res.* **100**, 22299–22314.

Pouchou, J.L., Pichoir, F., 1984. A new model for quantitative analyses. I. Application to the analysis of homogeneous samples. *Rech. Aérospat.* **3**, 13–38.

Pouchou, J.L., Pichoir, F., 1985. 'PAP' (ϕ–ρ–Z) correction procedure for improved quantitative microanalysis. In: Armstrong, J.T. (Ed.), *Microbeam Anal.*. San Francisco Press, San Francisco, pp. 104–106.

Révay, Zs., Belgya, T., Ember, P.P., Molnár, G.L., 2001. Recent developments in HYPERMET PC. *J. Radioanal. Nucl. Chem.* **248**, 401–405.

Révay, Zs., Belgya, T., Kasztovszky, Zs., Weil, J.L., Molnár, G.L., 2004. Cold neutron PGAA facility at Budapest. *Nucl. Instr. Meth. Phys. Res. B* **213**, 385–388.

Ridley, J., 1982. Arcuate lineation trends in a deep level, ductile thrust belt, Syros, Greece. *Tectonophysics* **88**, 347–360.

Ridley, J., 1984. Evidence for temperature-dependent 'blueschist' to 'eclogite' transformation in high-pressure metamorphism of metabasic rocks. *J. Petrol.* **25**, 852–870.

Ridley, J., 1986. Parallel stretching lineations and fold axes oblique to a shear displacement direction—a model and observations. *J. Struct. Geol.* **8**, 647–653.

Ring, U., Thomson, S.N., Bröcker, M., 2003. Fast extension but little exhumation: the Vari detachment in the Cyclades, Greece. *Geol. Mag.* **140**, 245–252.

Rosenbaum, G., Avigad, D., Sánchez-Gómez, M., 2002. Coaxial flattening at deep levels of orogenic belts: evidence from blueschists and eclogites on Syros and Sifnos (Cyclades, Greece). *J. Struct. Geol.* **24**, 1451–1462.

Ryan, J.G., 2002. Trace-elements systematics of beryllium in terrestrial materials. In: *Beryllium: Mineralogy, Petrology and Geochemistry*. In: Grew, E.S. (Ed.), *Rev. Mineral*, vol. 50. Mineral. Soc. Am., pp. 121–145.

Ryan, J.G., Langmuir, C.H., 1987. The systematics of lithium abundances in young volcanic rocks. *Geochim. Cosmochim. Acta* **51**, 1727–1741.

Ryan, J.G., Langmuir, C.H., 1988. Be systematics in young volcanic rocks: implications for ^{10}Be. *Geochim. Cosmochim. Acta* **52**, 237–244.

Ryan, J.G., Langmuir, C.H., 1993. The systematics of boron abundances in young volcanic rocks. *Geochim. Cosmochim. Acta* **57**, 1489–1498.

Sano, T., Hasenka, T., Shimaoka, A., Yonezawa, C., Fukuoka, T., 2001. Boron contents of Japan Trench sediments and Iwate basaltic lavas, Northeastern Japan: estimation of sediment-derived fluid contribution in mantle wedge. *Earth Planet. Sci. Lett.* **186**, 187–198.

Scambelluri, M., Müntener, O., Ottolini, L., Pettke, T.T., Vanucci, R., 2004. The fate of B, Cl and Li in subducted oceanic mantle and in the antigorite breakdown fluids. *Earth Planet. Sci. Lett.* **222**, 217–234.

Schmidt, M.W., Vielzeuf, D., Auzanneau, E., 2004. Melting and dissolution of subducting crust at high pressures: the key role of white mica. *Earth Planet. Sci. Lett.* **228**, 65–84.

Seck, H.A., Kötz, J., Okrusch, M., Seidel, E., Stosch, H.-G., 1996. Geochemistry of a meta-ophiolite suite: an association of metagabbros, eclogites and glaucophanites on the island of Syros, Greece. *Eur. J. Mineral.* **8**, 607–623.

Shaw, D.M., Higgins, M.D., Truscott, M.G., Middleton, T.A., 1988. Boron contamination in polished thin sections of meteorites: implications for other trace-element studies by alpha-track image or ion microprobe. *Am. Mineral.* **73**, 894–900.

Smith, H.J., Leeman, W.P., Davidson, J., Spivack, A.J., 1997. The B isotopic composition of arc lavas from Martinique, Lesser Antilles. *Earth Planet. Sci. Lett.* **146**, 303–314.

Sorensen, S.S., Grossman, J.N., Perfit, M.R., 1997. Phengite-hosted LILE enrichment in eclogite and related rocks: implications for fluid-mediated mass transfer in subduction zones and arc magma genesis. *J. Petrol.* **38**, 3–34.

Straub, S.M., Layne, G.D., 2002. The systematics of boron isotopes in Izu arc front volcanic rocks. *Earth Planet. Sci. Lett.* **198**, 26–39.

Szakmány, G., Kasztovszky, Zs., 2004. Prompt gamma activation analysis, a new method in the archeological study of polished stone tools and their raw materials. *Eur. J. Mineral.* **16**, 285–295.

Tenthorey, E., Hermann, J., 2004. Composition of fluids during serpentinite breakdown in subduction zones: evidence for limited boron mobility. *Geology* **32**, 865–868.

Tomascak, P.B., Widom, E., Benton, L.D., Goldstein, S.L., Ryan, J.G., 2002. The control of lithium budgets in island arcs. *Earth Planet. Sci. Lett.* **196**, 227–238.

Trotet, F., Jolivet, L., Vidal, O., 2001a. Tectono-metamorphic evolution of Syros and Sifnos islands (Cyclades, Greece). *Tectonophysics* **338**, 179–206.

Trotet, F., Vidal, O., Jolivet, L., 2001b. Exhumation of Syros and Sifnos metamorphic rocks (Cyclades, Greece). New constraints on the *P–T* paths. *Eur. J. Mineral.* **13**, 901–920.

Woodland, A.B., Seitz, H-M., Altherr, R., Olker, B., Marschall, H., Ludwig, T., 2002. Li abundances in eclogite minerals: a clue to a crustal or mantle origin? *Contribs. Mineral. Petrol.* **143**, 587–601, Erratum: Contribs. Mineral. Petrol. 144, 128–129.

You, C-F., Morris, J.D., Gieskes, J.M., Rosenbauer, R., Zheng, S.H., Xu, X., Ku, T.L., Bischoff, J.L., 1994. Mobilization of beryllium in the sedimentary column at convergent margins. *Geochim. Cosmochim. Acta* **58**, 4887–4897.

Zack, T., Rivers, T., Foley, S.F., 2001. Fluid infiltration at 2.0 GPa in eclogites from Trescolmen, Central Alps: constraints from Cs–Rb–Ba systematics in phengites and amphiboles. *Contibs. Mineral. Petrol.* **140**, 651–669.

Zack, T., Foley, S.F., Rivers, T., 2002. Equilibrium and disequilibrium trace element partitioning in hydrous eclogites (Trescolmen, Central Alps). *J. Petrol.* **43**, 1947–1974.

Zack, T., Tomascak, P.B., Rudnick, R.L., Dalpe, C., McDonough, W.F., 2003. Extremely light Li in orogenic eclogites: the role of isotope fractionation during dehydration in subducted oceanic crust. *Earth Planet. Sci. Lett.* **208**, 279–290.